Supporting Information

Visible-light driven water oxidation and oxygen production at soft interfaces

S1. Experimental Methods

S1.a. Chemicals

Butyronitrile (BCN, 99%), tetrabutylammonium tetrafluoroborate ($TBABF_4$, 99%) and chloride of potassium (KCl, ≥99%) were purchased from Acros, and $TCNQF_4$ was obtained from Sigma Aldrich. All aqueous solutions were prepared in MilliQ water (18.2 $M\Omega \cdot cm^{-1}$).

The standard gas bottles (0.8% O_2 - 99.2% $N_2$and 8.0% O_2) were obtained from Carbagas.

S1.b. Cyclic voltammetry

The cyclic voltammograms were recorder inside a glovebox with a PGSTAT 302N, Metrohm Autolab (Herisau, Switzerland) potentiostat. The solutions were placed in a glass cell using a commercial 3 mm diameter glassy carbon electrode or a Pt wire as working electrodes, Pt wire as counter electrode and an Ag/AgCl/3M KCl reference electrode. The scan rate was 50 $mV \cdot s^{-1}$.

S1.c. Gas Chromatographycoupled to Mass Spectrometry (GC-MS)

After the WOR, the headspace of the septum-sealed glass vials were sampled by using a lock-in syringe with a push−pull valve (SGE Analytical Sciences) and then analysed by injecting it into a Thermo Scientific Trace 1300 gas chromatograph. The column of the chromatograph was a 5Å molecular sieve, 80/100 mesh. Oxygen gas was detected using a mass spectrometry detector MSD employing Helium as gas carrier. A calibration curve was performed using O_2 standard gas (8% O_2 and 0.8% O_2), the oxygen of the air (21%) and the small amount of oxygen in the glovebox.

S1.d. UV-Vis absorption

UV-Visible absorption spectra of the $TCNQF_4$ and of samples taken during the photosensitized WOR were obtained by using a 10 mm optical path length quartz cell and a UV-Vis

Spectrometer (Agilent Technologies). All the solutions were diluted down to 0.0325 mM prior analysis.

S1.e. UV-Vis absorption

Dynamic light scattering analyses before and after the photosensitized WOR were performed using a 10 mm optical path length quartz cell and a Nano ZS Light Scattering equipment from Malvern at 633nm. All the samples were diluted down to 0.2 mM prior analysis.

S2. Electrochemical synthesis of $TCNQ^{-}$, and $TCNQ^{2-}$ and their UV-vis spectrums.

With the aim to determine by UV-visible which species are present after the reactions, $TCNQF_4^{-}$ and $TCNQF_4^{2-}$ were electrochemically synthesized to measure their corresponding UV-visible spectrums.

The electrochemical synthesis of $TCNQF_4^{-}$, and $TCNQF_4^{2-}$were carried out in an H-cell were the positive and negative side is separated by glass wool plug. This experimental setup allows separate the working from the counter electrode, in order to avoid the oxidation of $TCNQF_4^{-/2-}$ in the counter electrode. The negative side (cathodic compartment) was fill with 6mL $TCNQF_4$ 2mM and 100mM $TBABF_4$ as support electrolyte in BCN, and the positive side (anodic part) only with the supporting electrolyte. The counter and working electrodes were a Duocel® reticulated vitreous carbon, RCV, and an Ag/AgCl reference electrode.

Before the synthesis, a cyclic voltammograms at 25mV·s was recorder using a Glassy carbon as working electrode, in order to determine the potential for the reduction of $TCNQF_4$, as can be seen in Figure S1a. The potential of the electrochemical synthesis was set at 0.55V.vs.Ag/AgCl for the synthesis of $TCNQ^{-}$, and was set at -0.185 V.vs.Ag/AgCl to obtain $TCNQ^{2-}$ during 10 minutes under stirring. After that, the solutions obtained in the chatodic compartment of the H-cell were extracted and their UV-vis spectrum are shown in SI1b. As can be seen, all the species have different absorption spectrum. Neutral $TCNQF_4$ shows an absorption maximum at λmax=390nm, and $TCNQF_4^{\cdot-}$present a λ max at 413nm, and also other band at 755nm. Subhasis Panja et. al. obtained a similar spectrum in acetonitrile for $TCNQF_4^{1-}$. $TCNQF_4^{2-}$shows a λ max at lower wavelength, at λ max $\approx$335nm[1].

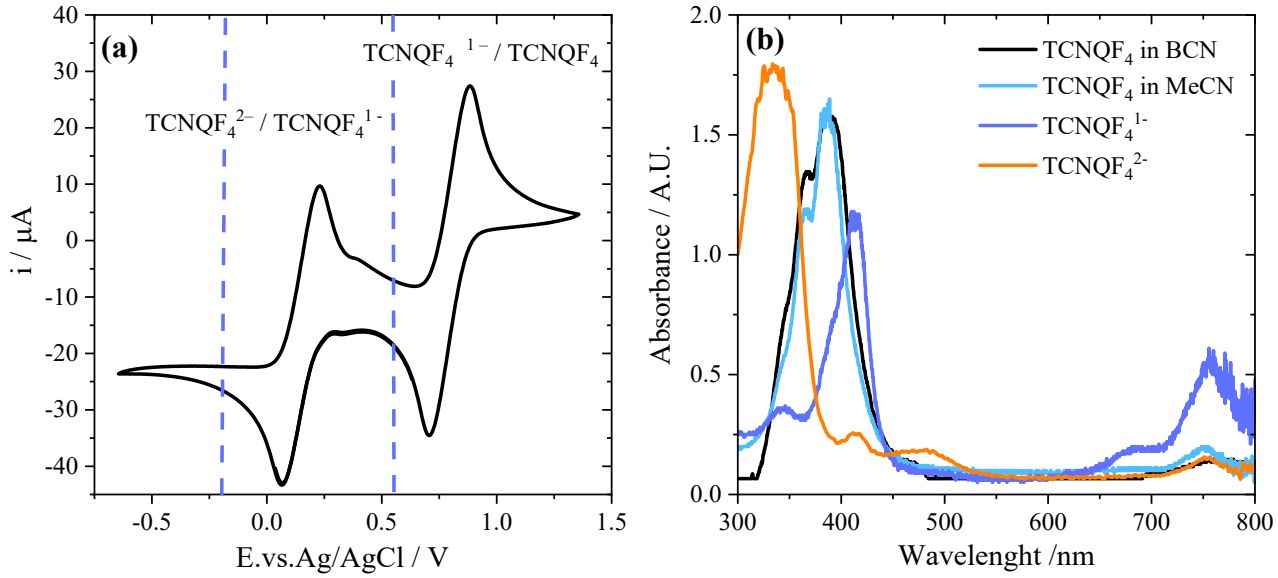

Figure S1. (a) Cyclic voltammogram of 4 mM TCNQF4 in 100 mM $TBABF_4$in dry BCN. A commercial 3 mm diameter glassy carbon electrode was used as working electrode, Pt wire as counter electrode and an Ag/AgCl 3M KCl as reference electrode. Scan rate 25 mV^{-1}.**(b)** UV-vis absorption spectra of 0,13mM of TCNQ, $TCNQF_4^-$ and $TCNQF_4^{2-}$.

S3. Optimization of the initial concentration of $TCNQF_4$

In order to verify the optimal concentration of $TCNQF_4$ to carry out the WOR, several experiments were carried out in which the initial concentration of $TCNQF_4$ varied and the obtained moles of O_2were determined after 60 minutes of reaction. As can be seen in Figure S2, using $TCNQF_4$ 2mM the highest amount of O_2 is obtained, and this variable was kept constant for all experiments.

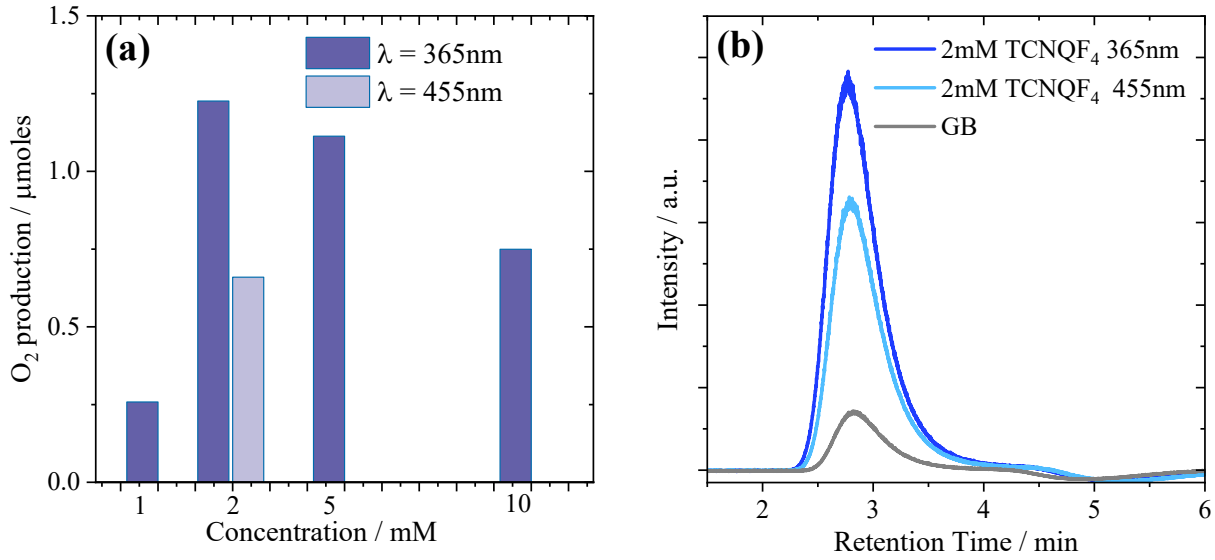

Figure S2. (a) Production of O_2 quantified after 60 minutes of WOR using different concentrations of $TCNQF_4$. **(b)** Chromatograms of the gas accumulated in the head space of the vessels after 60 minutes of WOR using 2mM $TCNQF_4$in the biphasic system employing the two different lamps.

S4. UV-vis and DLS of the biphasic and monophasic system using 455nm LED.

Figure S3a shows the UV-vis absorption spectra of the species present after different times of WOR using a 455nm LED in the biphasic systems. In this case, at short WOR times, the predominant species is $TCNQF_4^{2-}$. However, the band of the di-anionic molecule is highly stable, due to a slow WOR. Indeed, with the 455 nm LED the pH doesn't decrease as fast as when using the 365 nm LED. It is important to note that after 60 minutes of WOR, the band of the di-anionic molecule decreases and the band of the protonated molecule is better defined. The most important difference between 365 and 455nm LED is that even after 60 minutes of reaction using visible light, the band at 500nm attributed to the formation of $DCTC^-$ is hardly observed because O_2 production is not so high as compared to using the UV LED. For the DLS measurements, a similar behavior for both LED is observed.

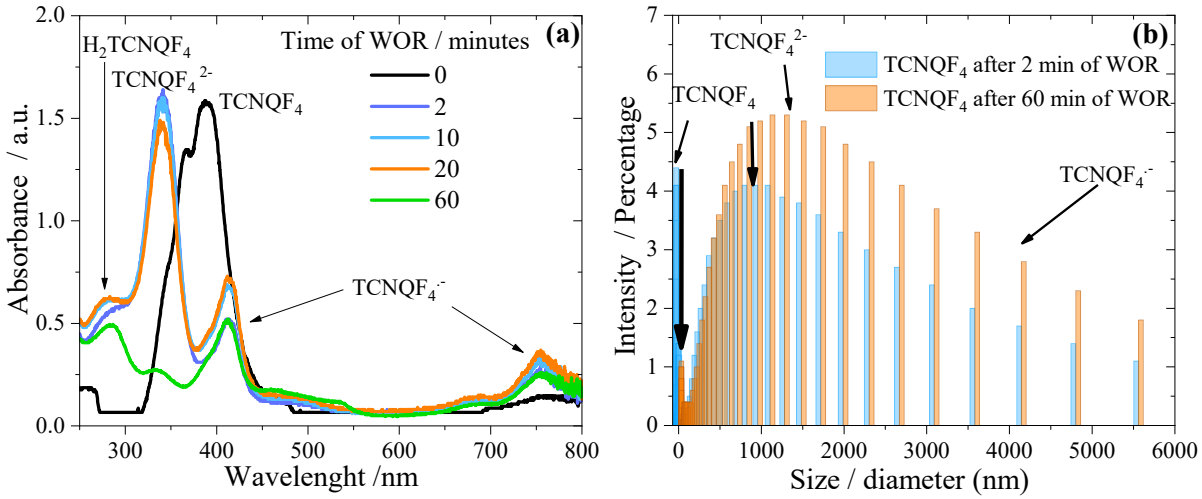

Figure S3. Analysis of the biphasic system (H_2O/BCN) after different times of WOR using 455nm led. **(a) UV-vis** absorption spectra of the organic phase containing 0.0325mM $TCNQF_4$ **(b)** DLS measurements of the organic phase after 2 and 60 minutes of WOR.

S5. DLS measurements of a solution of $TCNQF_4$ in BCN, and the organic phase after stirring the biphasic system without light.

It can be seen in Figure S4a that a solution of $TCNQF_4$ in BCN has an assembly of diameter of 10nm, as reported by Wouw et. al [2], it is equivalent to approximately 10 molecules of $TCNQF_4$, that is, an aggregate of 5 dimers. The reaction in dark shows small aggregates with diameter of approximately 35nm, which is inferior to the aggregates generated by the WOR using the 2 different LEDs. These aggregates of neutral $TCNQF_4$ can be increase in size by the stirring.

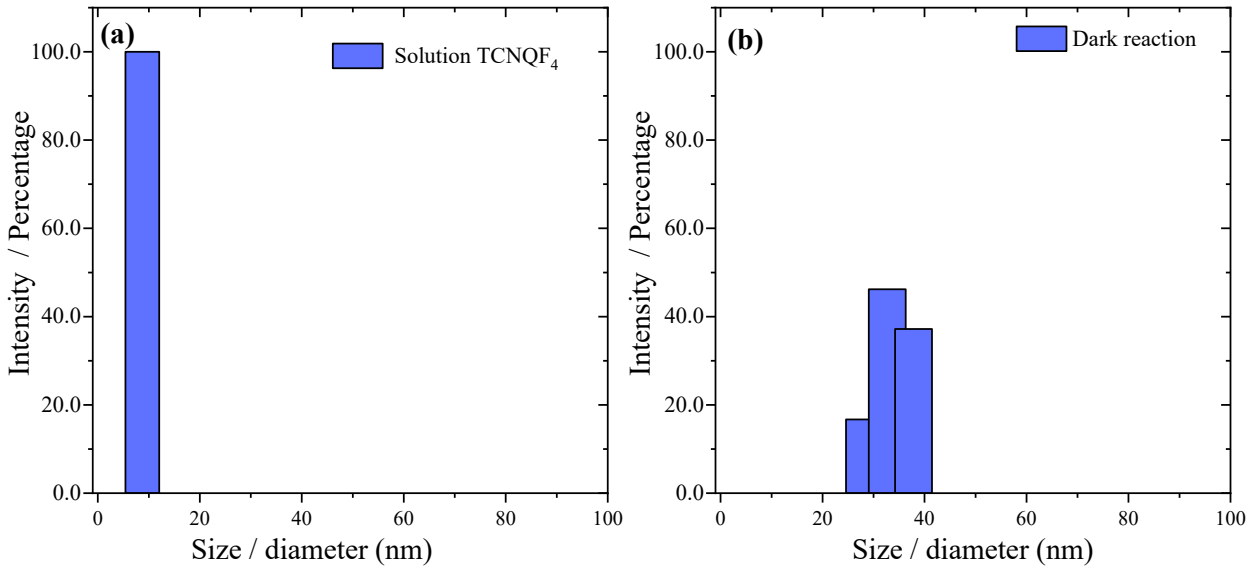

Figure S4. DLS of byphasic system **(a)** the fresh solution of $TCNQF_4$ and **(b)** organic phase of reaction carried out in dark.

S6. Production of O_2 after 60 minutes of WOR at different systems

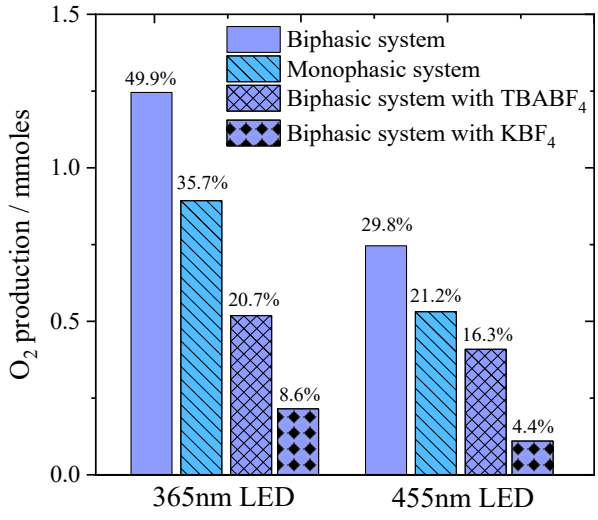

Figure S5. Production of O_2 quantified after 60 minutes of WOR using 2mM $TCNQF_4$ in biphasic, monophasic and when the electrolytes are added, up of the column the Y_{WOR} of each reaction are shown.

S7. DLS of the organic phase after WOR in the biphasic system with different electrolytes.

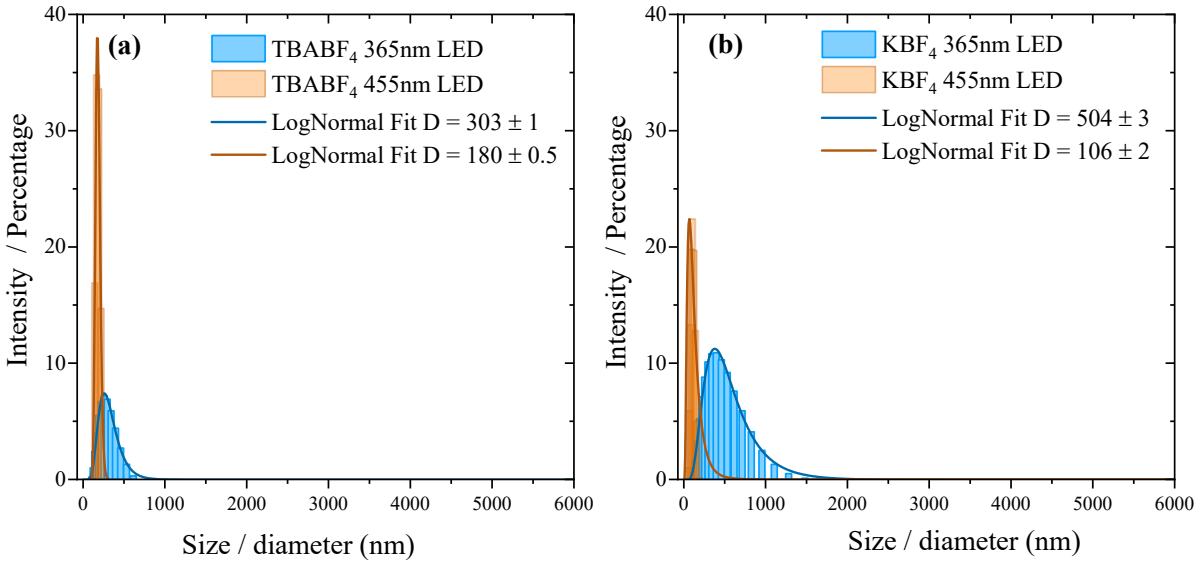

Figure S6. DLS measurements of the organic phase for two phases experiments using **(a)** $TBABF_4$ as electrolyte in the organic phase **(b)** KBF_4 as electrolyte in the aqueous phase after and 60 minutes of WOR.

S8. DLS of organic phase for the biphasic system after several days.

In order to clarify if the aggregates increase in size with the time, the DLS measurements were carried out again after 3 days and the results are shown in Figure S7. The size of the aggregates was the same as that obtained just after the WOR occurred, which shows that once these aggregates are formed, they do not grow any further.

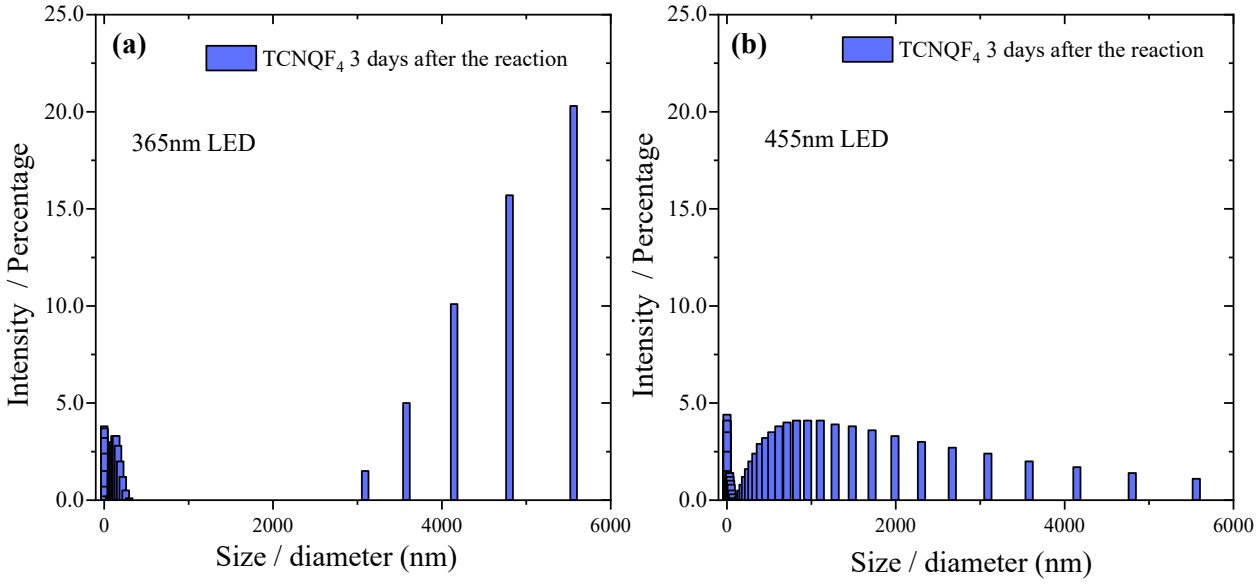

Figure S7. DLS of organic phase for the two phases experiments using **(a)** 365nm lamp and **(b)** 455nm lamp after 3 days of WOR.

S9. UV-vis spectrums and DLS measurement of the one phase experiments (Water/MeCN) using 365 and 455nm leds.

For the monophasic system, using the 365nm led, Figure S8a, the band of the neutral $TCNQF_4$ disappears immediately and the bands corresponding to $TCNQF_4^-$ and the protonated specie appear. Instead, using the 455 nm LED, Figure S8b, the band of the neutral $TCNQF_4$ species is observed after 20 minutes of WOR, indicating that the WOR with this LED is slower compared to the biphasic system.

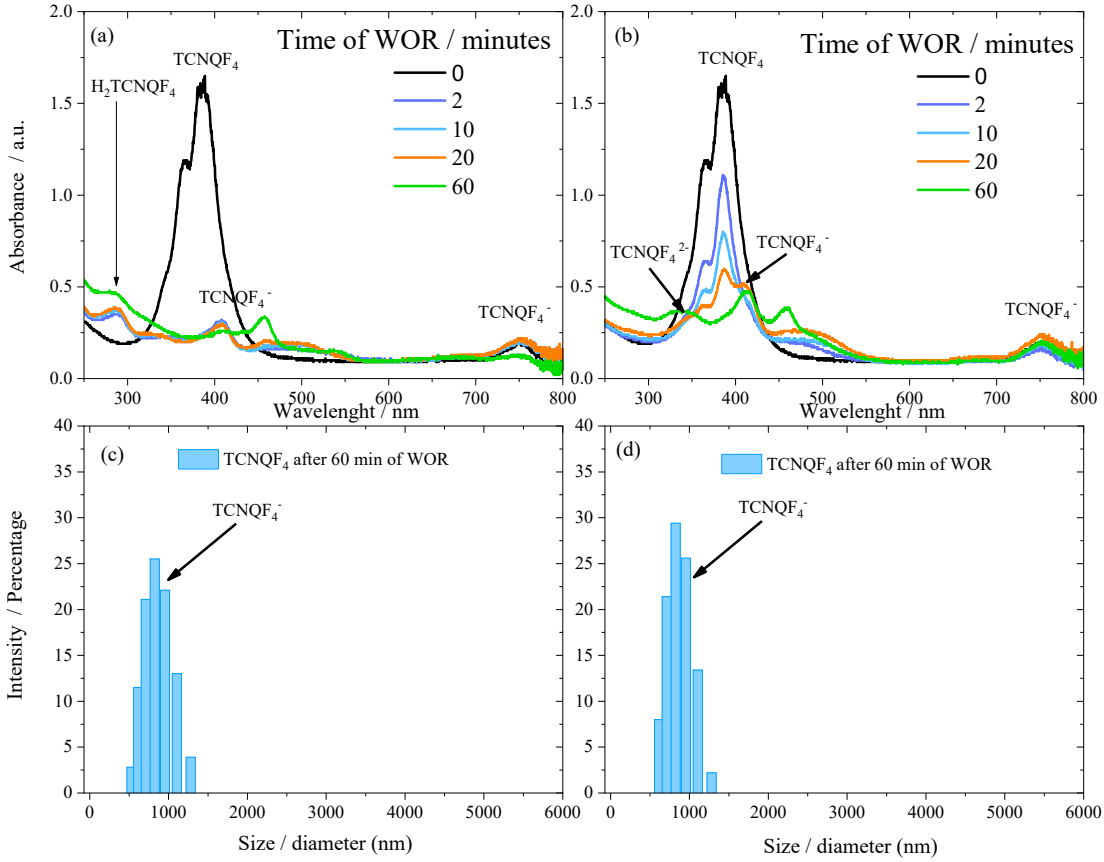

Figure S8.UV-vis absorption spectra of the organic phase containing 0.0325mM TCNQF4 at different time of reaction using **(a)** 365nm led (H_2O/MeCN), **(b)** 455nm led (H_2O/MeCN) and DLS measurements of the medium of reaction for monophasic experiments using **(c)** 365nm led and **(d)** 455nm led after 60 minutes of WOR.

For the DLS measurements, Figure S8d, the aggregates after the reaction are slightly larger than prior to the reaction, 880 nm with the 455 nm LED. For the monophasic system experiments, DLS measurements were also performed. As can be seen in Figure S8c and S8d, the aggregates after the reaction are a little bit larger than prior the reaction, 845nm for 365 LED and 826nm for 455 LED. Also it is observed that the aggregates in one-phase experiments have a smaller diameter than that for two-phase experiments.

S10. DLS measurements of a solution of $TCNQF_4$ in MeCN, and after stirring with water and without light.

Figure S9a shows that a fresh solution of $TCNQF_4$ in MeCN has an assembly of diameter around 300nm. The reaction in dark shows aggregates with a diameter of approximately 500 nm. This size is smaller than the aggregates produced after WOR, using 365nm or 455nm leds.

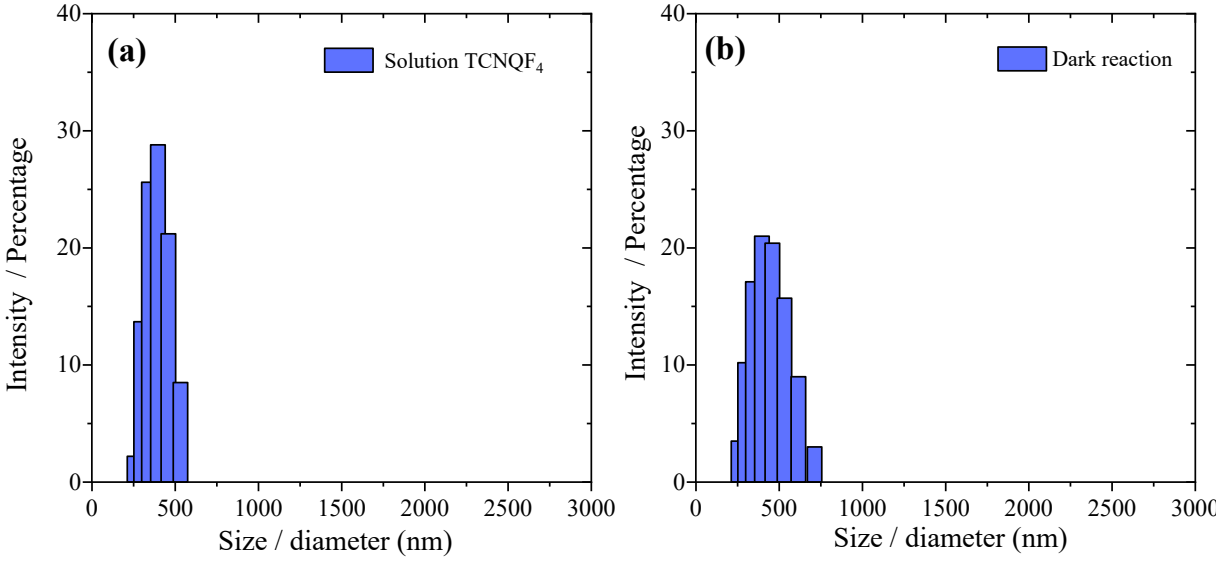

Figure S9. DLS of one phase experiments **(a)** the fresh solution of TCNQF4 and **(b)** reaction carried out in dark.

S11. Cyclic voltammograms of the aqueous and organic phases after photochemical WOR by $TCNQF_4$ using 365 and 455nm.

After WOR by $TCNQF_4$ and light in a water/BCN emulsion, the reaction cell was kept still and the aqueous and organic phases were separated. Each phase was analyzed by recording a cyclic voltammogram (CV) using a Pt electrode as a working electrode, a Pt wire as working electrode, and an Ag/AgCl/3M KCl as reference electrode. Potassium chloride KCl was added to the aqueous phase and $TBABF_4$ to the organic phase, both at a final concentration of 100mM to be used as support electrolytes. As can be seen in Figure S10a, when the CVs is recorded in the aqueous phase after the WOR, a reduction peak appear at –0.55V, which is attributed at the oxygen reduction reaction. Electrochemical reduction of oxygen involves one to four electron

transfers depending on conditions such as the solvent media and electrode material [3]. The electrochemistry of oxygen in water has been extensively studied, and the full four electron reduction to form water is possible on platinum electrodes[4]. Otherwise, when the CV is recorded with a glassy carbon (GC) electrode no peak is observed, which corroborates that the peak observed correspond to O_2 reduction reaction since glassy carbon electrode is not catalytic enough to O_2 reduction, and the concentration of O_2 after WOR could be not enough to be detected with a GC electrode.

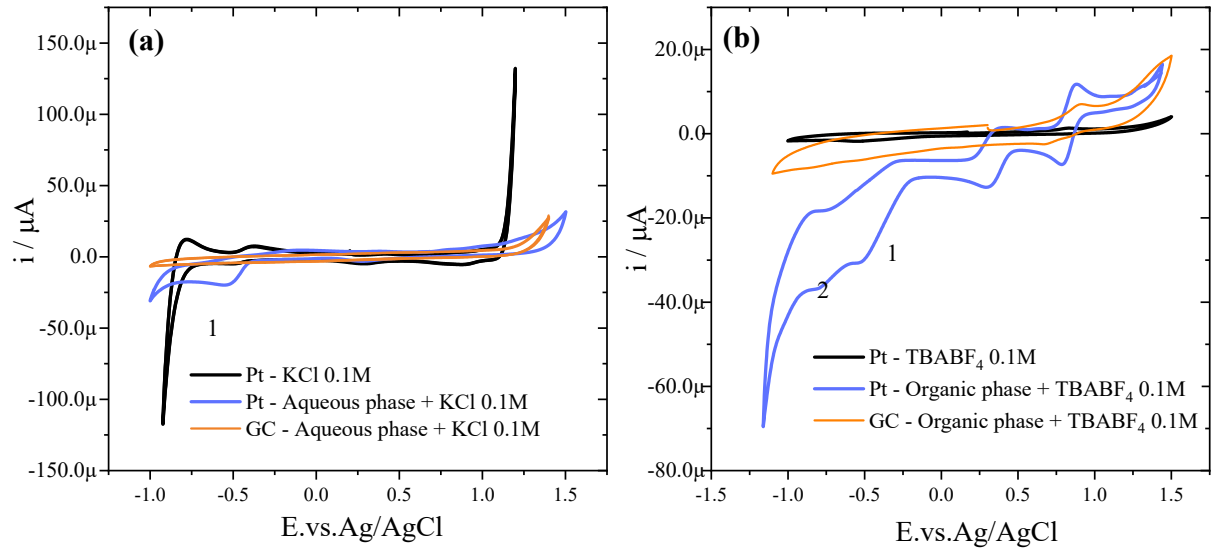

Figure S10. Cyclic voltammograms of aqueous **(a)** and organic **(b)** phases after 60 minutes of WOR. The **violet plot** corresponds to the CV using Pt as working electrode, **orange plot** corresponds to the CV using GC as working electrode and **black plot** corresponds to the CV of the blank using Pt as working electrode.

The first reduction peak corresponds to the formation of superoxide radical anion since it is usually stable in aprotic nonaqueous solvents, as N,N-dimethylformamide [5], dimethyl sulfoxide[6,7], acetone [8], and room-temperature ionic liquids [9-12], and acetonitrile (MeCN)[5,13], and can be formed on most electrode substrates following the equation 1 [14]:

$$O_2 + e^- \rightarrow O_2^{\cdot -} \quad (1)$$

$$2O_2^{\cdot -} + H_2O + e^- \rightarrow O_2 + HO_2^- + OH^- \quad (2)$$

$$2H_2O_2 + 2e^- \rightarrow H_2O \quad (3)$$

Then, the most probably reaction is a rapid disproportionation of $O_2^{\cdot-}$ to give oxygen and peroxide as is shown in eq. 2 in the presence of slight amount of water, as has been postulated for oxygen electroreduction in organic solvents [5,13].

Later, the second peak corresponds to the subsequent reduction of the peroxide to water, as shown in eq. 3. It should be noted that these two peaks are present after the WOR carried out illuminating both at 455nm or at 365nm (Figure S10). As shown for the aqueous phase, when a glassy carbon (GC) electrode is used to perform voltammetry in BCN, no reduction waves are observed, indicating clearly that the observed processes correspond to the O_2 reduction.

After 60 minutes of the WOR using 5mL of 2mM $TCNQF_4$ in BCN and 5mLwater, illuminating with a 365nm lamp and under vigorous stirring in order to make an emulsion, the cell was keep still for a while and each phase is spontaneously separated. The aqueous and the organic phase were separated in different cells and the supporting electrolyte was added before making the voltammogram.

Figure S11a shows the voltammogram obtained for the aqueous phase. It can be seen the same peak, corresponding to the O_2 reduction, that was shown after WOR illuminating with a lamp of 455nm (Figure S10a). Figure S11b shows the voltammogram obtained in the organic phase, similar to that obtained employing a lamp of 455nm.

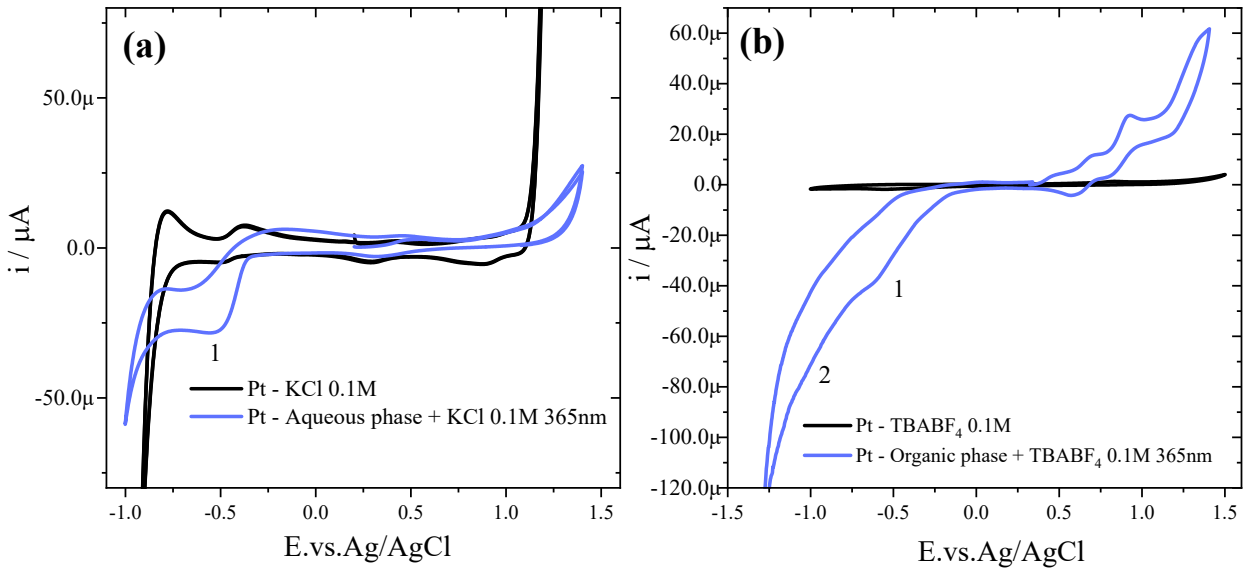

Figure SI11. Cyclic voltammogram of **(a)** Aqueous phase containing 100mM KCl in H_2O and **(b)** Organic phase containing 2 mM $TCNQF_4$ in 100 mM $TBABF_4$in dry BCN. A homemade Pt electrode was used as working electrode, Pt wire as counter electrode and an Ag/AgCl 3MKCl as reference electrode. Scan rate 50 mV^{-1}.

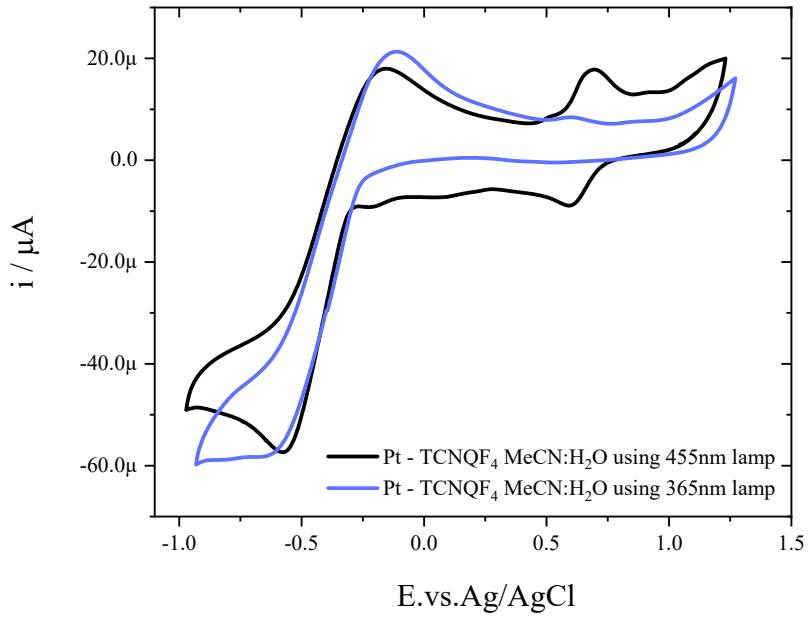

Figure S12. Cyclic voltammogram of **one phase experiments** phase containing 100 mM $TBABF_4$. A homemade Pt electrode was used as working electrode, Pt wire as counter electrode and an Ag/AgCl 3M KCl as reference electrode. Scan rate 50 mV^{-1}.

S12. Electron transfer reaction of $TCNQF_4$

As shown in scheme S1, $TCNQF_4$ can reacts with one or two electrons to form the anion and dianion molecule. When the $TCNQF_4^{2-}$ is exposed to O_2, a oxidation reaction occurs to produce an α,α-diciano-*p*-toluoilcianuro anion ($DCTC^-$), which shows a band at ~500nm in the absorption spectrum[15].

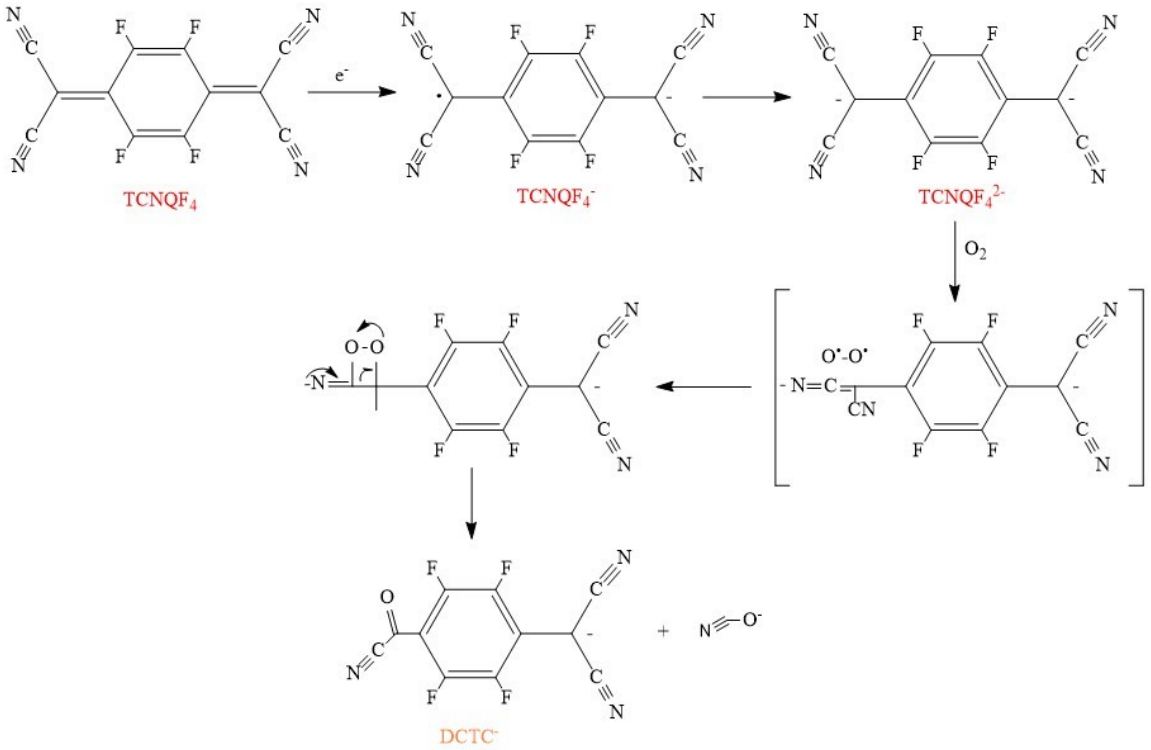

Scheme S1. Electron transfer reaction of $TCNQF_4$ and oxidation reaction of $TCNQF_4^{2-}$ by O_2.

S13: Formation and reaction of H_2O_2 with $TCNQF_4$

To verify the formation of H_2O_2 upon WOR the aqueous phase was separated, treated with an excess of NaI and analyzed by UV/Vis spectroscopy. The I_3^- formation would indicate the oxidation of I^- by H_2O_2. I_3^- was not detected, indicating that H_2O_2 was not present in the aqueous phase, which is to be expected considering that the acidic pH, and illumination strongly favours the decomposition of H_2O_2 to water and O_2. Additional controls also showed that H_2O_2 can be rapidly reduced by $TCNQF_4^{2-}$. Therefore, at the conditions of the experiment the formation of H_2O_2 cannot be neither corroborated, nor discarded experimentally.

Two control experiments in a biphasic system using 1mM H_2O_2 as aqueous phase, with 2mM $TCNQF_4$ in the organic phase were realized. One experiment was carried out with irradiation at 365nm and the other without irradiation. After 10 minutes, 100 µL of the aqueous phase were put in contact with 2mL of NaI 0.2M and a UV-vis spectrum was recorder as shown below. From these control experiments, we can conclude that H_2O_2 reacts with $TCNQF_4$ and for this reason, we can not discard mechanism 2.

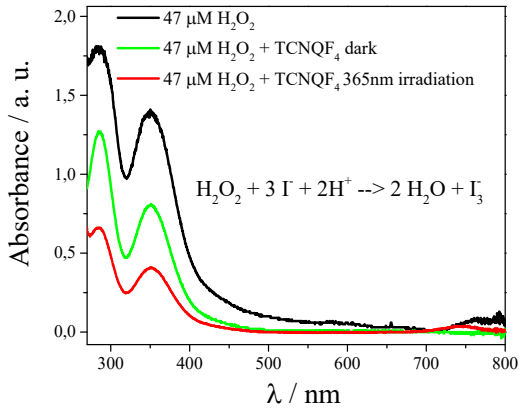

Figure S13. UV-vis spectrum of I_3^- after the reaction of NaI with 47µM H_2O_2 and $TCNQF_4$ with 365nm irradiation for 10 minutes and without irradiation.

S14: Computational details

Calculations were performed at the M062X[16]/6-31G* level using the Gaussian 09 suite of programs,[17] M06-2X functional was chosen since it has demonstrated to be suitable for describing non-bonding interaction.[18] Solvent effect was considered though IEFPCM model as implemented in g09 using acetonitrile as continuous solvent. The compounds (monomers and dimers) were optimized, and all structures were confirmed as minima by Hessian matrix calculations. The binding energies were estimated at M062X/6-311G*//M062X/6-31G* level, as a difference between energy of a given dimer and the sum of energies of isolated components including zero-point vibrational energies.

Cartesian coordinates corresponding to dimers

Neutral-neutral dimer (TCNQF4-TCNQF4)

40 scf done: -2150.302107

C	-0.812900	-1.779128	-0.995588
C	0.533414	-1.754700	-1.043613
C	1.300587	-0.529372	-0.902186
C	0.497940	0.673383	-0.777750
C	-0.848138	0.648888	-0.733435
C	-1.612594	-0.583141	-0.796590
C	2.669538	-0.513064	-0.864849
C	-2.972575	-0.619023	-0.644843
C	3.454082	0.683741	-0.741028
N	4.156444	1.598007	-0.645535
C	3.477938	-1.700713	-0.898213
N	4.188317	-2.614138	-0.872883
C	-3.787894	0.548401	-0.456663
N	-4.512338	1.437794	-0.306997
C	-3.734767	-1.836707	-0.613857
N	-4.405707	-2.776835	-0.541034
F	1.120347	1.838073	-0.682764
F	-1.504824	1.790505	-0.598366
F	-1.436262	-2.940191	-1.129997
F	1.187033	-2.892709	-1.225362
C	-0.351467	-4.189401	2.567384
C	0.994617	-4.164771	2.523186
C	1.758912	-2.932656	2.586080
C	0.959071	-1.736679	2.784493
C	-0.387266	-1.761159	2.831783
C	-1.154292	-2.986695	2.691254
C	3.118910	-2.896693	2.434174
C	-2.523252	-3.003281	2.654199
C	3.880976	-1.678940	2.402509
N	4.551683	-0.738696	2.329009
C	3.934344	-4.064083	2.246304
N	4.658975	-4.953346	2.096777
C	-3.331760	-1.815670	2.686847
N	-4.042283	-0.902368	2.661193
C	-3.307708	-4.200271	2.531739
N	-4.009953	-5.114743	2.437391
F	1.582302	-0.575510	2.918801
F	-1.040908	-0.623118	3.013166
F	1.651392	-5.306342	2.388174
F	-0.973746	-5.354159	2.472370

Nautral- ANION dimer (HTCNQF4-TCNQF4)

41 scf done: -2151.128528

C	0.146878	-0.307669	0.123287
C	0.094286	-0.423753	1.506065
C	1.238728	-0.405794	2.281182

C	2.531498	-0.243541	1.741608
C	2.564769	-0.159386	0.330617
C	1.420360	-0.182195	-0.437381
F	-1.083143	-0.593381	2.118303
F	1.095616	-0.580977	3.604131
C	3.701706	-0.211320	2.564540
C	3.654200	0.091136	3.949046
N	3.668733	0.352478	5.083579
F	3.736630	-0.004918	-0.295661
F	1.525080	-0.049436	-1.764104
C	-1.113771	-0.204259	-0.710403
C	-1.195747	1.103668	-1.395563
N	-1.247125	2.133972	-1.912656
C	5.011048	-0.335575	2.038845
N	6.107659	-0.460522	1.669075
C	-1.225699	-1.293218	-1.700551
N	-1.325116	-2.165411	-2.449961
C	-0.246479	-4.982791	-1.877561
N	0.049920	-5.349096	-2.934776
C	-0.707676	-4.570216	-0.583161
C	-2.119616	-4.753192	-0.412363
N	-3.264087	-4.917895	-0.353424
C	0.122173	-4.082848	0.397142
C	-0.326426	-3.791733	1.743324
C	0.520021	-3.445183	2.737823
C	1.949506	-3.323228	2.540082
C	2.374909	-3.481594	1.166067
C	1.531515	-3.838017	0.174797
F	-1.617694	-3.924390	2.021438
F	0.030755	-3.254764	3.955495
C	2.838410	-3.096234	3.563746
C	2.438351	-2.876527	4.924445
N	2.195755	-2.697031	6.041795
F	3.649029	-3.250236	0.873088
F	2.007618	-3.952495	-1.059213
C	4.264139	-3.184455	3.414502
N	5.415538	-3.305415	3.388568
H	-1.982662	-0.281757	-0.044693

References

1. S.Panja,U.Kadhane, J.U.Andersen, A.I.S.Holm, P. Hvelplund, B.S. Kirketerp, S. Nielsena andK. Støchkel, *J. Chem. Phys.*2007, **127**, 124301.

2. H.L.Van de Wouw; J.Chamorro, M. Quintero andR.S. Klaussen, *J. Chem. Educ.* 2015, **92**, 12, 2134–2139.

3. Sawyer, D.T.; Sobkowiak, A.; Roberts, J.J.L. Electrochemistry for Chemists, second ed., John Wiley and Sons, Inc., **1995.**

4. Yeager, E. Electrocatalysts for O_2 reduction. Electrochim. Acta 29, **1984**, 1527-1537.

5. Vasudevan, D.; Wendt, H. Electroreduction of Oxygen in Aprotic Media. *J. Electroanal. Chem.* 392, **1995**, 69–74.

6. Sawyer, D.T.; Chlerlcato, G.; Angells C.T.; Nannl, E.J.; Tsuchlya, T. Effects of Media and Electrode Materials on the Electrochemical Reduction of Dioxygen. Anal. Chem. **1982**, 54, 1720-1724.

7. Wadhawan, J.D.; Welford, P.J.; Maisonhaute, E.; Climent, V.; Lawrence, N.S.; Compton, R.G.; McPeak, H.B.; Hahn, C.E.W. Microelectrode Studies of the Reaction of Superoxide with Carbon Dioxide in Dimethyl Sulfoxide. J. Phys. Chem. B **2001**, 105, 43, 10659–10668.

8. Wei, Y.; Shao, C.; Hufeng. Voltammetric Response an Electrochemical properties of the $O_2/O^{\cdot-}_2$ couple in Acetone. Russ. J. Electrochem. 43, **2007**, 178.

9. Huang, X.J.; Rogers, E.; Hardacre, C.; Compton, R.G.The Reduction of Oxygen in Various Room Temperature Ionic Liquids in the Temperature Range 293−318 K: Exploring the Applicability of the Stokes−Einstein Relationship in Room Temperature Ionic Liquids. *J. Phys. Chem. B* **2009**, 113, 26, 8953–8959.

10. Evans, R.G.; Klymenko, O.V.; Saddoughi, S.A.; Hardacre, C.; Compton, R.G. Electroreduction of Oxygen in a Series of Room Temperature Ionic Liquids Composed of Group 15-Centered Cations and Anions. *J. Phys. Chem. B* **2004**, 108, 23, 7878–7886.

11. Buzzeo, M.C.; Klymenko, O.V.; Wadhawan, J.D.; Hardacre, C.; Seddon, K.R.; Compton, R.G. Voltammetry of Oxygen in the Room-Temperature Ionic Liquids 1-Ethyl-3-methylimidazolium Bis((trifluoromethyl)sulfonyl) imide and Hexyltriethylammonium Bis((trifluoromethyl)sulfonyl)imide: One-Electron Reduction To Form Superoxide. Steady-State and Transient Behavior in the Same Cyclic Voltammogram Resulting from Widely Different Diffusion Coefficients of Oxygen and Superoxide. *J. Phys. Chem. A* **2003**, 107, 42, 8872–8878.

12. Jacob, S.R.; Hong, Q.; Coles, B.A.; Compton, R.G. Variable-Temperature Microelectrode Voltammetry: Application to Diffusion Coefficients and Electrode Reaction Mechanisms. *J. Phys. Chem. B* **1999**, 103, 15, 2963–2969.

13. Lorenzola, T.A.; Lopez, B.A.; Giordano, M.C. Molecular Oxygen Electroreduction at Pt and Au Electrodes in Acetonitrile Solutions. J. Electrochem. Soc. 130, **1983**, 1359–1365.

14. Li, Q.; Batchelor-McAuley, C.; Lawrence, N.S.; Hartshorne, R.S.; Compton, R.G. Anomalous Solubility of Oxygen in Acetonitrile/Water Mixture Containing tetra-n-butylammonium perchlorate Supporting Electrolyte; The Solubility and Diffusion Coefficient of Oxygen in Anhydrous Acetonitrile and Aqueous Mixtures. *J. Elec. Chem* 688, **2013**, 328–335.

15. Ning, X.; Li; Y.; Ming, J.; Wang, Q.; Wang, H.; Cao, Y.; Peng, F.; Yang, Y.; Yu, H. Electronic synergism of pyridinic- and graphiticnitrogen on N-doped carbons for the oxygen reduction reaction. Chem. Sci., **2019**, 10, 1589.

16. Y. Zhao and D. G. Truhlar, *Theor. Chem. Acc.* 2008, **120**, 215-41.

17. M. J. Frisch, et al, Gaussian 09, Revision D.01, Gaussian, Inc., Wallingford, CT, USA, 2009.

18. N. Mardirossian, M. Head-Gordon, *J. Chem. Theory Comput*. 2016, **12**, 4303−4325.